Ranges and Energy-Loss Processes of Heavy Ions in Emulsion*

Harry H. Heckman, Betty L. Perkins, William G. Simon, Frances M. Smith, and Walter H. Barkas
Lawrence Radiation Laboratory, University of California, Berkeley, California
(Received August 12, 1959)

The range-energy relations for C, N, O, Ne, and A ions in nuclear-track emulsion have been measured for energies up to 10 Mev/nucleon. The ions, accelerated by the heavy-ion linear accelerator, were suitably degraded and subsequently analyzed by a 180° double-focusing magnetic spectrometer. The heavy-ion ranges were measured relative to those of alpha particles which were employed to calibrate the instrument. Within the energy interval studied, it has been found that a general expression for the range of a heavy ion is $R = (M/z^2)\lambda(\beta) + Mz^{\frac{1}{3}}C_z(\beta/z)$, where $\lambda(\beta)$ is the range of a particle of proton mass and charge at velocity βc, $C_z(\beta/z)$ is an empirical function that corrects for the extension in range caused by neutralization of the ionic charge as electrons are captured at low velocities, and M and z are the ionic mass and charge in units of the proton. The range data are sufficiently complete and accurate to allow detailed analyses of rates of energy loss and effective charge of the heavy ions as they come to rest. The relative importance of primary and secondary ionization processes in producing the taper in the track of a multicharged ion has been studied by examining the ions in emulsions of various sensitivities. Buckling-type distortions of heavily ionizing tracks in strongly developed emulsions are also discussed. The range-energy relation for low-velocity protons is re-examined and an improved range point at 0.585 Mev is reported.

I. INTRODUCTION

THE heavy-ion linear accelerator (Hilac) of this Laboratory has been successful in accelerating useful beams of carbon, nitrogen, oxygen, neon, and argon ions to energies of 10.4±0.2 Mev/nucleon. In order to effectively utilize these beams, range calibration data are required. We have been led to carry out a systematic study of the range-energy relations for ions of charge $6 \leqslant z \leqslant 18$. The results of this experiment have enabled us to deduce a generalized range-energy relation for an ion of mass M and charge z in units of the proton.

The first range measurements of ions heavier than He[4], principally Li[6,7,8] and B[8], were obtained by detecting the ions as secondary reaction products in nuclear-track emulsion.[1-4] Miller extended these measurements by using cyclotron-accelerated C[12] ions of 120 Mev.[5] Nitrogen ranges in emulsion have been studied by Reynolds and Zucker between 5 and 30 Mev,[6] and by Chaminade *et al.* between 10 and 100 Mev.[7] More recently, Parfanovich *et al.* have published range-energy relations for nitrogen and oxygen ions in Ilford $E1$ emulsions in the interval from 3 to 120 Mev.[8] Preliminary results also have been reported by Roll and Steigert on range-energy work undertaken at Yale University.[9] Aside from the ranges of fission fragments no experimental information on ranges of ions heavier than oxygen has heretofore been published for emulsion.[10]

In the velocity interval with which we are concerned, i.e., $\beta(=v/c)$ up to 0.148, the conditions for the validity of the Bethe-Bloch theory of stopping are seriously violated. The condition is not satisfied that the velocity of the ion be well above the velocity of the fastest electron in the stopping material. The theory of stopping of heavy ions is further complicated by the fact that as the ion approaches the velocity of its own K electrons, it will begin to neutralize itself by picking up electrons. The ions will therefore have a monotonically decreasing average effective charge with decreasing velocity and will be completely neutralized by the time they reach the end of their range. The lack of an exact theory has necessitated an essentially semiempirical approach for the calculation of heavy-particle ranges. The calculations that have been made[11-14] take as a basis the results obtained by Knipp and Teller in their theoretical calculations for the range and energy-loss of heavy ions in air.[15]

Assuming a Fermi-Thomas model of the atom, Knipp and Teller proposed that the degree of ionization be given by

$$z'/z = f(v_e/z^{\frac{2}{3}}),$$

where $z' =$ charge carried by the ion, $z =$ nuclear charge, and $v_e =$ velocity of the least-bound electron. A modified Bohr criterion,[16] namely that the capture and loss

* This work was performed under the auspices of the U. S. Atomic Energy Commission.
[1] Neuendorffer, Inglis, and Hanna, Phys. Rev. **82**, 75 (1951).
[2] P. Cüer and J. P. Lonchamp, Comp. rend. **232**, 1824 (1951).
[3] H. Faraggi, Compt. rend. **229**, 1223 (1949).
[4] W. H. Barkas, Phys. Rev. **89**, 1019 (1953).
[5] James F. Miller, University of California Radiation Laboratory Report UCRL-1902, July, 1952 (unpublished).
[6] H. L. Reynolds and A. Zucker, Phys. Rev. **96**, 393 (1954).
[7] Chaminade, Crut, Faraggi, Garin-Bonnet, Olkowsky, and Papineau, Compt. rend. **242**, 105 (1956).
[8] Parfanovich, Semchinova, and Flerov, J. Exptl. Theoret. Phys. (U.S.S.R.) **33**, 343 (1958) [translation: Soviet Phys. JETP **6**(33), 266 (1958)].
[9] P. G. Roll and F. E. Steigert, Bull. Am. Phys. Soc. **4**, 51 (1959).

[10] An initial report of this work was presented at the American Physical Society meeting, December 1958 [H. H. Heckman *et al.*, Bull. Am. Phys. Soc. **3**, 419 (1958)].
[11] J. P. Lonchamp, J. phys. radium **14**, 89 (1953).
[12] J. J. Wilkins, Atomic Energy Research Establishment, Harwell Report G/R-664, 1951 (unpublished).
[13] D. L. Livesey, Can. J. Phys. **34**, 203 (1956).
[14] A. Papineau, Commissariat à l'Energie Atomique Report CEA-543, 1956 (unpublished).
[15] J. Knipp and E. Teller, Phys. Rev. **59**, 659 (1941).
[16] N. Bohr, Phys. Rev. **58**, 654 (1940).

cross sections are equal when $v_e = \gamma v_{ion}$, was adopted by Knipp and Teller, where γ is an adjustable parameter near unity to be determined by experiment. It has been shown, however, that γ is not a constant, but for nitrogen ions may vary inversely with velocity between values of 0.65 and 1.1,[17] while for fission fragments in air, values as high as 1.7 are found.[15]

Papineau[14] has utilized the experimental results[17-20] of the charge distributions of N, O, and Ne ions up to 2 Mev/nucleon to construct an empirical curve of the ratio of ion charge to maximum charge as a function of the reduced velocity, $\beta/z^{\frac{2}{3}}$. A unique locus seems to be defined independent of the stopping material or the ion atomic number. By extrapolating these data to higher (and lower) velocities, the range curves for ions of $3 \leqslant z \leqslant 10$ were calculated for energies up to 10 Mev/nucleon.

II. EXPERIMENTAL PROCEDURE

A schematic diagram of the experimental arrangement is shown in Fig. 1. The magnet is a 180° double-focusing ($n = 0.5$) spectrometer of 18-in. radius. At a peak field of about 20 kilogauss, the maximum $B\rho$ is 9.2×10^5 gauss-cm. The source was defined by a $\frac{1}{16}$-in. wide slit and the vertical and horizontal deviations of the beam in the magnet were limited by a $\frac{1}{4} \times \frac{3}{8}$-in. collimator, giving a momentum resolution less than 0.1% at the focal point of the system.

To lower the beam energy, the ions were passed through a wedge-shaped target. Actually the wedge was a series of three conical holes placed in a "thick" 10-mil Al foil with a $\frac{1}{16}$-in. wire drill. The beam, upon traversing this type of degrader, had a continuous momentum spectrum from zero to the peak momentum of the accelerated beam. As the velocity of a multicharged ion is reduced, it tends to pick up orbital electrons. The degraded beam, for this reason, consisted of ions in various charge states from $z' = 0$ to the atomic number z. Since the magnetic rigidity, $B\rho$, was determined by the geometry and magnetic field, only particles with discrete values of $pc = z'eB\rho$ were transmitted by the spectrometer. The emulsion detectors therefore recorded particles whose ranges fell into separated and well-defined groups corresponding to the discrete momenta, $(e/c)B\rho z'$, transmitted by the spectrometer.

After the wedge degrader was bombarded, it was replaced by a 10-mil Al absorber, called the alpha target. This target was thick enough to stop the primary beam, though thin enough to allow secondary alphas and protons produced in the target and emitted in the forward direction to be recorded by the detectors. From the measured ranges of the alpha particles and their range-energy relation in emulsion, the $B\rho$ of the par-
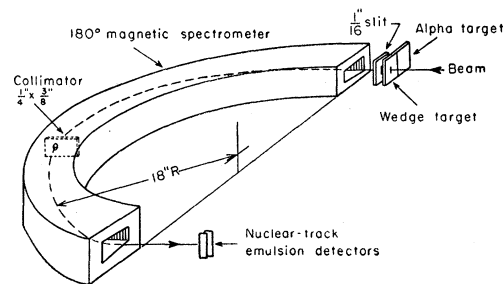

FIG. 1. Experimental arrangement.

ticles was determined. The energies of the separate range groups of the heavy ions could then be calculated, once the charge of each range group was determined.

Ilford emulsions of type $C2$ were used in the experiment. The emulsions were 50 microns thick, 1×3-in. glass-backed plates, all from the same batch. The density of the emulsions at about 60% humidity is generally taken to be 3.815 g/cm³. However, when emulsions are placed in vacuum, as in this experiment, their density cannot be well defined until equilibrium with respect to their moisture content is reached.[21] To insure a uniform density during exposure, the emulsions were dried in atmospheres of 30 to 0% relative humidity for a period of 3 to 4 days prior to their use. The time the emulsions were in vacuum before exposure was typically 20 minutes. Completely dry emulsion has a density of 4.01 g/cm³. We estimate that at the time of exposure the emulsion density was $4.00_{-0.03}^{+0.01}$ g/cm³, but because of the range-ratio measurement procedure employed our results are not sensitive to the emulsion density.

As shown in Fig. 1, the 3-in. dimension of each plate was positioned normal to the median plane of the magnet and rotated to allow the particles to enter at a 6 to 8° dip. Exposed in this manner, all tracks recorded on a particular plate had essentially the same momentum. The resolution in momentum was calculated to be better than 0.1%, with a gradient of about 0.2%/mm. As the particles entered the emulsion surfaces at about 6° dip, the dispersion appears on each plate as a momentum gradient of about 0.2%/cm along the particle direction. The average magnetic field during a run was maintained constant to a few parts in 10^4 and the ripple was less than one part in 10^4.

III. RANGE MEASUREMENTS AND CORRECTIONS

Before extensive range measurements were undertaken, various technical problems needed to be resolved. Since the ranges of the heavy ions and alpha particles were all less than 200 microns and 500 microns, respectively, the measurements were most easily done with calibrated eye-piece reticles. Precision reticles were specially made and checked for uniformity. Vari-

[17] Reynolds, Scott, and Zucker, Phys. Rev. **95**, 671 (1954).
[18] Reynolds, Wyly, and Zucker, Phys. Rev. **98**, 474 (1955).
[19] K. G. Stephens and D. Walker, Phil. Mag. **45**, 543 (1954).
[20] E. L. Hubbard and E. J. Lauer, Phys. Rev. **98**, 1814 (1955).

[21] A. Oliver, Rev. Sci. Instr. **25**, 326 (1954).

ations in uniformity were found to be less than 0.1%. More serious, however, was the problem of selecting objectives that possessed uniform magnification within the limits of the measuring reticle. Track lengths of about 25 reticle units (full scale=100 r.u.) showed variations of apparent range up to 0.5% in some cases. The distortions were most often symmetric about the optical axis, but not in all cases. In the objectives finally selected, no distortions of this type were detectable.

To eliminate scanner subjectivity in the range measurements, a rigid definition of an operational range was made. Provided the track had an unambiguous entrance point, no detectable scatter, and no blob-type ending, the measured range was defined as the distance between the tangents to the extremities of the first and last grains of the track. The true range of a particle is found by applying two corrections to this measured range:

(a) A mean grain diameter (0.46±0.05 micron) must be subtracted, since on the average a heavily ionizing particle traverses only about one-half of the first and last grains of the track, and the swelling of the grains on development is assumed to be symmetric. This correction was applied to both the heavy-ion and alpha-particle ranges.

(b) In the case of a lightly ionizing particle, an additional correction must be made to take into account the most probable distance the particle penetrates the emulsion before rendering a grain developable. The additive correction to be made for this effect is given by

$$\Delta = \langle G \rangle L, \qquad (1)$$

where L is the lacunarity or mean linear fraction of the track that consists of gaps, and $\langle G \rangle$ is the mean gap length. This correction was measured for the alpha particles but found to be negligible, i.e., less than 0.02 μ.

The striking characteristics of a heavy-ion track in emulsion are the track width and its taper as it comes to rest in emulsion. As we shall discuss later, the broadening of the tracks is due primarily to the production of δ rays along the track. The effect is most readily observed in electron-sensitive emulsions, types $G5$ or $K5$, although the tapering effect is still apparent in the less sensitive emulsions $C2$ and $L2$. Although it was believed that the true ranges of the heavy ions would be the same in emulsions of different sensitivities, there was the possibility that our measured ranges would not be independent of emulsion sensitivity. This was suggested to us when we observed that about 1% of the tracks had an identifiable δ ray scattered in the backward direction near the point where the ion entered the surface of the emulsion (δ-ray production is largely limited to the angular interval of 90° and less to the beam direction). Let us assume that the track width depends on a mean "diffusion" distance of the δ rays from the core of the track. This point of view suggests the possibility that there may be a direct correlation

between the track length and initial track width (and therefore emulsion sensitivity), since any diffusion backward could systematically extend the measured range.

This problem was investigated by measuring particle ranges in emulsions of widely different sensitivities, K minus 2, $K0$, $D1$, and $G5$.[22] The emulsions were exposed simultaneously to the full-energy beams of all the ion types. The mean ranges of the ions for each emulsion type were corrected for end effects and normalized to the ranges of carbon ions (which have fewest δ rays) to eliminate any differences of emulsion densities. No systematic differences of the ranges were detected, as a function of either emulsion sensitivity or of atomic number of the ion. The average statistical accuracy of the normalized mean ranges was 0.3%. To within these errors, we conclude that the backward diffusion of δ rays from the point of entry is not statistically an important effect in our range measurements. The probability of such a δ ray occurring is small, and when it does, it is detected as a single δ ray and the track is rejected by the criterion that the entrance point must be well defined.

A further possible uncertainty in defining the point of entry has been considered. When emulsion is made, each crystal is surrounded by a protective envelope of gel that adheres to the crystal. The extreme surface layer of the emulsion is consequently pure gel which must be traversed by the charged particle before any crystal can be penetrated. Fast, heavily ionizing particles, however, produce δ rays in the gel. The δ rays render developable silver halide crystals that are adjacent to the point of entry of the particle even if the crystals are not penetrated by the particle. It seems therefore that little or no correction should be made for this effect, and we have made none.

IV. ANALYSIS AND RESULTS OF RANGE MEASUREMENTS

Each plate was independently scanned by two observers. The scanning was done back and forth across the beam direction and proceeded symmetrically toward the edges of the emulsions from the center of the plate. The observer was instructed, first, to measure all tracks that fulfilled the selection criteria until 50 events were recorded in each range group or until the entire beam area was searched; and second, to measure 50 or more calibrating alpha particles. Fundamentally, our measurements are of relative ranges, i.e., heavy-ion ranges relative to the alpha-particle range at the same $B\rho$. It is from this viewpoint that the raw data were handled. The quantities that were evaluated from each plate were the ratios $\bar{R}_{z'}/\bar{R}_\alpha$, where $\bar{R}_{z'}$ refers to the (true) mean range of the heavy-ion range group that carried charge z' in the magnetic field, and $\bar{R}_\alpha$,

the (true) mean range of the alpha particles. The results of the two measurements from a single plate were statistically weighted and combined to give the final mean ratio.

There are several advantages in using the ratio method. First, any systematic differences in reticle calibration of the microscopes are eliminated; second, the ratios $\bar{R}_{z'}/\bar{R}_\alpha$ are slowly varying with velocity; and third, the adjustments of the ratios to standard emulsion density are small. The density correction is velocity-dependent,[23] and thus the correction factor required to adjust the ratios to standard conditions depends upon the relative velocity of the ion and the alpha particle. In the magnetic field, completely stripped C, N, O, and Ne ions, with $z'/M = \frac{1}{2}$, have the same velocity as alpha particles, and the density correction is zero. The average correction for all ratios was less than 0.2%; the maximum amounted to 3.2%. (The latter density correction was made to the very short argon ranges.) It should be understood that (although the emulsion employed in this experiment had a density of about 4.00 g/cm³) all ranges are given for standard emulsion of density 3.815 g/cm³. After all corrections were made to the data, the energies of the alpha particles were determined from their absolute ranges and the relativistic energies of each heavy-ion range group calculated.

Figure 2 shows the range spectra obtained from the six separate exposures to neon ions. The $B\rho$ of the spectrometer for each run was deduced from the alpha-particle ranges. This series of exposures was typical in that the changes in $B\rho$ between adjacent runs were small enough to allow for an overlap in the ranges. At the highest velocities, $\beta \approx 0.148$, the ions are predominantly stripped of electrons and the assignment of $z' = 10$, for Ne, to the group of maximum range is clearly justified. In the overlapping regions, the charge-state assignments could be internally checked because at equal ranges the momenta are equal and $z_1'(B\rho)_1 = z_2'(B\rho)_2$. Since charge equilibrium of the ions is reached after they have passed through about 20 μg/cm² of matter (0.05 μ in emulsion), no detectable difference is expected in the ranges of ions having equal momenta but carrying different charges in the magnetic field.

In principle, the accuracy of the relative measurements was limited only by the number of events used to determine the ratios $\bar{R}_{z'}/\bar{R}_\alpha$. The absolute accuracy of a single range-energy point, however, is actually limited by the range-energy relation used to evaluate the alpha-particle energies from their ranges. This error is most probably between 0.2 and 0.3%. The range straggle of the ions introduced by the finite momentum resolution of the spectrometer was in all cases a fraction of the calculated range straggle experienced by the particles in coming to rest in the emulsion. For long ranges of alpha particles, the observed range straggling
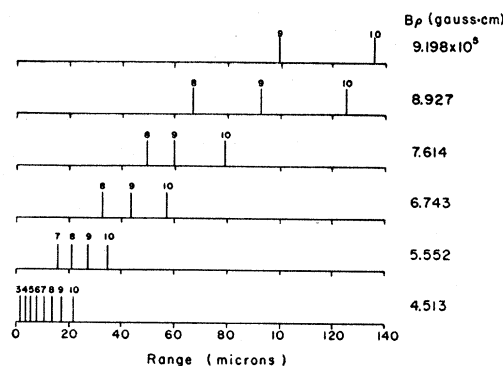

FIG. 2. Range spectra for neon ions obtained from the six emulsion exposures at different values of $B\rho$. Alpha particles served to calibrate the spectrometer. The charge carried by the ion in the magnetic field is indicated for each range group.

agreed closely with the theoretical expected value of 0.7 to 0.8%.[24] If one calculates in a similar fashion the expected straggling for the heavy ions, the result is about 0.4%. The straggling actually observed was seldom less than 1.0%. The reasons for this discrepancy can be attributed to other processes of energy loss, such as elastic atomic collisions, statistical fluctuations in the charge carried by the ion in coming to rest, the heterogeneity of the emulsion, and the dispersion of the range measurements due to the finite grain size of the emulsion. For ranges less than 20 μ, the latter effect produced an irreducible standard deviation of the range distribution of about ± 0.2 μ, one-half the mean diameter of the developed grain. As the velocity of the ion decreases, the energy loss by ionization diminishes and the primary energy-loss process becomes that of non-ionizing atomic collisions. The contributions to the range straggling of the ions for these energy-loss mechanisms occur for velocities $\beta < 1/137$, i.e., for residual ranges of several microns. We do not expect this to produce observable effects, however, as any additional straggling at these ranges would be masked by the finite grain size of the emulsion.

We have already mentioned that the absolute accuracy of our range-energy measurements is primarily limited by the accuracy of the range-energy relation we use to evaluate the mean energies of the calibrating α particles. In connection with this research, a new investigation of the very low-energy proton range-energy curve was carried out. The range-energy relation at high velocities was recently studied extensively.[23,25] The best information then available for protons below 1 Mev was found to be consistent with a rate of energy loss varying in inverse proportion to the particle velocity. The initial part of the range curve was roughly defined on this assumption. Emulsion data from the literature are difficult to interpret because

[23] Barkas, Barrett, Cüer, Heckman, Smith, and Ticho, Nuovo cimento 8, 185 (1958).

[24] W. H. Barkas, University of California Radiation Laboratory Report UCRL-2579 Rev., September, 1954 (unpublished).
[25] W. H. Barkas, Nuovo cimento 8, 201 (1958).

TABLE I. Range-energy relation and rates of energy loss for a particle of proton mass.[a]

τ (Mev)	λ (μ)	ι (Mev/cm)	τ (Mev)	λ (μ)	ι (Mev/cm)
0.1	0.99	1500	5.0	175.9	172
0.2	1.78	1130	6.0	237.9	151
0.3	2.76	950	7.0	307.8	136
0.4	3.91	820	8.0	385.3	123
0.6	6.69	650	9.0	470.3	113
1.0	13.92	490	10.0	562.5	104
1.5	25.63	380	11.0	662.0	97.1
2.0	40.01	316	12.0	768.5	90.9
3.0	76.43	244	13.0	882.0	85.5
4.0	121.9	201	14.0	1002.4	80.7

[a] Below 2.0 Mev the ranges have been determined from differential stopping-power data. The ranges 2.0 Mev and greater have been reduced by about 0.4 μ from those given in reference 25 to correct for the finite grain size of the initial and terminal grains of the track. This correction also brings the two sets of data into agreement at 2.0 Mev.

often the emulsion density is poorly known and the method of making the end corrections (if any) is seldom discussed. In view of the complications introduced by the emulsion granularity, and for these other reasons, it was decided to consider differential energy-loss measurements made in pure substances.

Ward Whaling kindly supplied us with a preprint of his report.[26] This paper reviews numerous measurements of the energy losses of low-energy particles in penetrating various materials. The empirical data are so complete that it has been found possible to graph, for fixed values of the proton velocity, the electronic stopping cross section as a function of atomic number. A family of continuous curves is found in this way. Except at the lowest velocities, the curves are smooth. Since the data came from more than one source, this smoothness probably indicates that they are reliable. Furthermore, the low-velocity irregularities seem to follow a pattern having the same periodicity as the chemical properties of the elements.

With these data one can, of course, add the stopping effects of all the emulsion constituents at each velocity and thus obtain the rate of energy loss for protons as a function of their velocity. Failure of this additivity of atomic cross sections in predicting stopping cross sections of molecules exists, and it is important at low velocities. For protons of less than 150 kev, as a rule, additivity does not hold, but above this energy the failure of additivity could not be detected by Reynolds et al. except for NO.[27] Integration of the rate of energy-loss data can be carried down to about $\tau = 0.1$ Mev. One empirical range-energy point then suffices to establish the range-energy relation. This normalization is discussed below.

The range data thus derived for proton energies less than 2.0 Mev are included in Table I, which presents the range-energy relation we have adopted for Ilford

[26] W. Whaling, in Handbuch der Physik, edited by S. Flügge (Springer-Verlag, Berlin, 1958), Vol. 34, p. 193.
[27] Reynolds, Dunbar, Wenzel, and Whaling, Phys. Rev. 92, 742 (1953).

emulsion of standard composition and density. The curve of λ vs τ joins smoothly to the high-energy curve[25] ($\tau \geqslant 2.0$ Mev) when one allows for the fact that the earlier values of λ were not corrected for the granularity. The notations λ (range in microns) and τ (energy in Mev) are the same as in reference 25, and are the range and energy for an "ideal" particle of protonic mass. (An ideal particle is one that behaves like a negative μ meson in that at low velocities it has neither a high capture cross section nor a tendency to capture orbital electrons.)

The true range, R, and energy, T, for a particle of mass M (in units of the proton mass) and atomic number z at any velocity β (which specifies λ and τ) are given by

$$R = R_{obs} - R_c = \rho[(M/z^2)\lambda + R_{ext}], \qquad (2)$$

$$T = M\tau. \qquad (3)$$

Here R_{obs} is defined as the mean distance between the extremities of the first and last developed grains of the track; R_c is the term that accounts for (a) the finite size of the fiducial and terminal grains of the track, and (b) (for lightly ionizing particles) the most probable distance the particle penetrates the emulsions before rendering a grain developable. If tracks are known to originate in the gel phase of the emulsion or enter through the surface, the correction R_c is about equal to $D - \Delta$, where D is the mean developed grain diameter. When the point of origin of the track is known to be a star-center or similar well-defined point, no correction is made for the fiducial end of the track; and the R_c term becomes simply $+D/2$, the correction for the strongly ionized terminus of the track. The quantity ρ is a factor (generally near unity) required to adjust the ranges measured in emulsion of nonstandard composition to their equivalents in standard emulsion.[23] The range of the particle would be $M\lambda/z^2$ if no end effects of high capture cross section, granularity, or sensitivity affected the measurement, and if the particle did not capture electrons at low velocities. The quantity R_{ext} is the correction term necessary to account for the extension in range of the positive ion owing to electron pickup in coming to rest. It is a function only of z at high velocities, but for velocities β comparable to $z/137$ and below, electron capture causes R_{ext} to become a function of velocity. Of course, it approaches zero as the velocity vanishes.

In order to study R_c and obtain an absolute range point, measurements of short tracks produced by particles of known energy are useful. When a range is short it can be measured with small absolute error; therefore tracks of low-energy protons are desirable for the normalization. Ilford $G5$ and $C2$ plates that had been exposed to thermal neutrons were obtained through the kindness of Dr. Glenn M. Frye and Dr. A. H. Armstrong of the Los Alamos Scientific Laboratory and Dr. F. C. Gilbert of the Lawrence Radiation Labora-

tory, Livermore. In these plates, the tracks from the reaction $N^{14}(n,p)C^{14}$ were measured. The reaction energy is 0.627 ± 0.001 Mev; the kinetic energies of the carbon and proton are 41.8 kev and 0.585 ± 0.001 Mev, respectively. The track length measured in the emulsion was actually the sum of the C^{14} and proton ranges. The mean distances between the extremities of the track in the $G5$ and $C2$ plates at 40% relative humidity were found to be 7.600 ± 0.065 and $7.118 \pm0.056\ \mu$, respectively. The straggling in each case was 4.5% (standard deviation).

To determine the range R of the proton, an estimate must be made of the C^{14} range plus *one* mean grain diameter (to correct for the terminal grains of the carbon and proton tracks) which is to be subtracted from the measured track lengths. The range of a C^{14} ion with kinetic energy 41.8 kev in air at NTP is ≈ 0.03 cm.[28] The stopping power of the gel must be much the same as of air when expressed in Mev/g. In silver halide, at this velocity, the range (in microns) will be about the same as in the gel.[12] These considerations lead one to estimate that the recoil C^{14} ion will have a range of $0.3\pm0.1\ \mu$. Since the mean distance between crystals is less than $0.2\ \mu$ in each emulsion type, it may be assumed that the carbon ion penetrates at least one silver halide crystal after it originated in the gel phase of the emulsion. The mean grain diameter was taken to be $0.68\ \mu$ for $G5$ emulsion and $0.35\ \mu$ for type $C2$. After making these corrections and adjusting the ranges to standard density (a $+1.1\%$ range correction) we obtain, for the proton range, $R=\lambda+R_{\text{ext}}$, $6.69\pm0.12\ \mu$ in $G5$, and $6.54\pm0.12\ \mu$ in $C2$. The difference of $0.15\pm0.09\ \mu$ is not statistically significant, but because of the possibility of a remaining sensitivity effect, we shall adopt the $G5$ range. If the R_{ext} of the proton is taken to be $0.12\ \mu$,[29] then we have $\lambda=6.57 \pm0.12\ \mu$ at $\tau=0.585\pm0.001$ Mev.

For our analysis of the heavy-ion range data, we require an accurate range-energy relation for alpha particles for kinetic energies greater than about 8 Mev (i.e., $\tau>2$ Mev) from Eqs. (2) and (3). The values of λ given in Table I for τ between 2 and 14 Mev were calculated from a least-squares-fit polynomial, of type $\log_{10}\lambda=\sum_{n=0}^{2} a_n[\log_{10}\tau]^n$, to the data of reference 25. This analytical function served as an interpolating function in this limited energy region. The coefficients are $a_0=1.1343$, $a_1=1.5276$, and $a_2=0.08820$. To evaluate the alpha range, R, we have taken the R_{ext} of the α particle to be $1.2\pm0.2\ \mu$. We give a detailed discussion of the R_{ext} term as it pertains to heavy ions in general in the next section of this paper.

The range-energy relation for alpha particles as calculated from Eqs. (2) and (3) was compared with Wilkins's range curves for alphas.[12] It was found that the two range-energy curves agreed to within an average

of 0.2% between the energies of 0 and 30 Mev (i.e., $\tau=2$ to 7.5 Mev) after Wilkins's range data were adjusted from his density of 3.92 to the adopted density of 3.815. In the region of $\tau=10$ Mev the curves differ by about 1%, although at $\tau=13.94$ Mev the $\lambda-\tau$ curve has been verified to be correct to 0.21%.[30] We have assumed an average error of 0.2% in λ for estimating the errors of the experimental results; where we have internal checks, this figure appears to be justified.

Table II, columns (a), (b), and (c), summarizes the corrected experimental range measurements. The results are grouped in the same order in which they were compiled from each run. Column (c) is the standard deviation of each range measurement. The error, $\sigma(\mu)$, takes into account statistical errors of the range measurements, the $\lambda-\tau$ relation (0.2%), the error in R_{ext} of the alpha, and errors in the correction factors applied to the ranges for mean-grain-diameter and mean-gap-length effects of the order of $0.07\ \mu$.

To be able to present the results in a more useful form, a polynomial of type $R=\sum_0^k a_k(T)^k$ was adjusted to give a weighted least-squares fit to the range data for each heavy ion. To insure proper behavior at zero energy, the range at this point was taken to be $0.00\pm0.05\ \mu$, where the error is the uncertainty in the measurement of the mean grain diameter. The computations were carried out on an IBM-650 computer until the residuals, $R_{\text{obs}}-R_{\text{cal}}$, were approximately equal to the statistical errors of the measurement. The residuals are included in Table II, column (d), for purposes of comparison with the errors of the observations. The rms value of the ratio $(R_{\text{obs}}-R_{\text{cal}})/\sigma(\mu)$ for all points is 1.2. The value of 1.00 would be obtained, on the average, if the external and internal errors were equal, so that the magnitudes of the errors have not been much underestimated or any serious error overlooked.

The smoothed range-energy data are given in Table III. The increments in energy have been chosen small enough so that errors in linear interpolation between adjacent entries are less than $0.05\ \mu$. Although the data cannot be represented with sufficient accuracy by a set of range curves, Fig. 3 is given to summarize graphically the experimental results. The solid curves are the least-squares curves; the dots are the observed points.

V. RANGE EXTENSION DUE TO CHARGE PICKUP AND A GENERALIZED RANGE-ENERGY RELATION

The problem of describing in detail the energy-loss processes of multicharged ions in matter, which would lead to a theoretical range-energy relation, is formidable. For this reason we have little or no theory sufficiently refined for comparison with our results. In an attempt to generalize the range data, we have defined the range R for a particle of mass M and charge z to be given by

[28] See for example Evans, Stier, and Barnett, Phys. Rev. **90**, 825 (1953).
[29] W. H. Barkas, Phys. Rev. **89**, 1019 (1953).

[30] Gilbert, Heckman, and Smith, Rev. Sci. Instr. **29**, 404 (1958).

TABLE II. Experimental range-energy measurements for C^{12}, N^{14}, O^{16}, Ne^{20}, and A^{40} ions.[a]

Run	(a) T(Mev)	(b) $R(\mu)$	(c) $\sigma(\mu)$	(d) $R_{obs} - R_{calc}$	Run	(a) T(Mev)	(b) $R(\mu)$	(c) $\sigma(\mu)$	(d) $R_{obs} - R_{calc}$
		Carbon					Neon		
1	113.4	180.3	0.44	0.74	1	203.1	135.5	0.31	−0.78
	78.89	101.2	0.28	−0.17		164.7	99.45	0.30	−0.65
2	66.01	77.53	0.20	−0.12	2	191.2	124.9	0.31	0.34
	45.88	46.25	0.15	−0.11		155.0	92.22	0.23	0.42
3	53.34	57.23	0.17	0.12		122.6	66.70	0.19	0.39
	37.06	34.96	0.12	0.06	3	139.4	78.99	0.20	−0.11
	23.73	20.42	0.11	0.37		113.0	59.53	0.17	0.03
4	43.66	43.35	0.14	−0.07	4	109.43	57.04	0.19	0.00
	30.33	27.03	0.10	0.02		88.68	43.42	0.15	−0.20
	19.42	15.86	0.11	−0.02		70.10	32.75	0.13	−0.12
5	29.41	26.08	0.11	−0.02	5	73.51	34.75	0.12	−0.05
	20.43	16.89	0.09	0.07		59.57	27.34	0.10	0.20
	13.08	10.44	0.09	0.04		47.08	20.83	0.10	−0.05
6	9.40	7.61	0.08	0.04		36.05	15.64	0.12	−0.17
	6.53	5.35	0.08	−0.04	6	49.00	21.78	0.10	−0.03
	4.18	3.65	0.08	0.07		39.70	17.42	0.10	−0.02
						31.37	13.74	0.08	−0.02
		Nitrogen				24.02	10.69	0.09	0.07
1	133.5	160.3	0.39	0.64		17.65	7.93	0.08	0.00
	98.20	100.0	0.26	0.14		12.26	5.54[b]	0.10	−0.08
2	97.51	98.67	0.25	−0.19		7.85	3.62[b]	0.15	−0.06
	71.71	63.18	0.17	−0.36		4.41	1.92[b]	0.10	−0.18
3	76.69	70.02	0.19	0.20					
	56.38	46.00	0.13	0.16			Argon		
4	51.58	40.67	0.13	−0.11	1	329.4	81.84	0.24	−0.17
	37.91	27.68	0.11	−0.14		293.9	71.06	0.21	0.05
5	40.18	29.86	0.12	0.02		260.5	61.17	0.18	−0.03
	29.53	20.88	0.10	0.10		229.0	52.45	0.17	−0.05
	20.52	13.75	0.11	−0.10	2	309.7	75.74	0.19	−0.08
	13.13	9.26	0.18	0.46		276.4	65.89	0.18	0.10
						244.9	56.89	0.16	0.06
		Oxygen				215.3	48.94	0.14	0.08
1	153.0	145.3	0.36	−0.26		187.6	41.74	0.15	−0.06
	117.3	97.27	0.24	−0.01	3	177.4	39.12	0.14	−0.15
	86.23	64.09	0.49	0.74		158.2	34.75	0.14	0.01
2	88.77	65.41	0.17	0.12		140.2	30.60	0.11	0.03
	68.04	45.59	0.14	−0.06		123.2	26.85	0.10	0.07
	50.02	31.27	0.25	0.20		107.4	23.37	0.09	0.00
3	39.88	23.84	0.10	0.09		92.61	20.34	0.09	0.01
	30.54	17.64	0.09	−0.01		78.92	17.55	0.09	−0.07
	22.45	12.82	0.09	−0.03		66.33	15.28	0.09	0.08
	15.59	9.02	0.09	0.01		54.82	12.96	0.09	0.00
	9.98	5.91	0.09	0.00		44.41	10.89	0.15	−0.02
	5.61	3.33[b]	0.12	−0.10		35.10	9.05	0.16	0.06
					4	37.09	9.16[b]	0.13	−0.25
						30.04	7.74[b]	0.11	−0.16
						23.74	6.47[b]	0.19	0.00
						18.17	4.93[b]	0.20	−0.19
						13.35	3.46[b]	0.35	−0.43
						9.27	2.47[b]	0.25	−0.31

[a] The ranges are grouped in the same order as observed in each emulsion plate. The ranges for each run are listed in the order of decreasing charge state carried by the ion in the magnetic spectrometer. The maximum range group in each run is that of the fully stripped ions, except for argon run No. 4 with $z_{max}' = 10$.

[b] *Note added in proof.*—Great reliance must not be placed on the indicated numbers because the resolution of these range groups could not be made with complete certainty.

Eq. (2). Figure 4 gives the extensions in range of the ions, R_{ext}, owing to charge pickup as a function of $(M/z^2)\lambda(\beta)$. The quantity $(M/z^2)\lambda$ would be the range of the ions if there were no neutralization of charge in coming to rest. It is clear that only the carbon and nitrogen ions have reached their maximum range extensions of 8.45 and 11.1 μ, respectively, while oxygen, neon, and argon remain partially neutralized at the highest obtainable velocities.

If one takes as the independent variable, $137 \beta/z$, the velocity in units of the K-electron velocity, it is found that the data given in Fig. 4 can be well represented by a unique function when the ordinate is taken to be $R_{ext}/Mz^{\frac{2}{3}} \equiv C_z$ (Fig. 5). Thus, within the velocity interval of the experiment, the results of the range-energy measurement can be generalized by the expression

$$R_{obs}(\beta) - R_c = R = (M/z^2)\lambda(\beta) + Mz^{\frac{2}{3}}C_z(\beta/z), \quad (4)$$

where $R_{obs}(\beta)$ = measured (operational) range, R_c = end corrections to measured range, R = "true" range, $\lambda(\beta)$ = proton range at velocity β, C_z = value of function for

TABLE III. Heavy-ion ranges (in microns) in Ilford emulsion of density 3.815 g/cm³.[a]

T(Mev)	C¹²	N¹⁴	O¹⁶	Ne²⁰	A⁴⁰	T(Mev)	C¹²	N¹⁴	O¹⁶	Ne²⁰	A⁴⁰
4	3.44	2.86	2.48	1.91	1.25	176				110.3	38.94
8	6.50	5.49	4.80	3.75	2.42	180				114.0	39.92
12	9.58	8.08	7.03	5.51	3.53	184				117.7	40.90
16	12.85	10.69	9.23	7.23	4.58	188				121.5	41.89
20	16.42	13.49	11.46	8.92	5.58	192				125.4	42.88
24	20.31	16.45	13.74	10.61	6.53	196				129.3	43.89
28	24.53	19.55	16.10	12.32	7.44	200				133.3	44.90
32	28.93	22.79	18.56	14.03	8.33	204					45.93
36	33.60	26.16	21.14	15.78	9.18	208					46.96
40	38.56	29.68	23.83	17.58	10.01	212					47.99
44	43.80	33.35	26.64	19.42	10.83	216					49.04
48	49.32	37.18	29.56	21.32	11.62	220					50.09
52	55.12	41.22	32.53	23.28	12.41	224					51.15
56	61.20	45.42	35.63	25.30	13.19	228					52.22
60	67.56	49.79	38.84	27.38	13.98	232					53.30
64	74.21	54.33	42.17	29.51	14.75	236					54.39
68	81.13	59.03	45.61	31.70	15.52	240					55.48
72	88.34	63.90	49.16	33.94	16.29	244					56.58
76	95.83	68.94	52.83	36.15	17.06	248					57.69
80	103.6	74.14	56.61	38.44	17.84	252					58.81
84	111.6	79.51	60.51	40.79	18.62	256					59.94
88	120.0	85.04	64.51	43.20	19.41	260					61.07
92	128.6	90.74	68.64	45.66	20.21	264					62.21
96	137.5	96.60	72.87	48.18	21.02	268					63.36
100	146.7	102.6	77.22	50.75	21.83	272					64.52
104	156.1	108.8	81.68	53.38	22.66	276					65.69
108	165.9	115.2	86.26	56.06	23.50	280					66.86
112	175.9	121.7	90.95	58.81	24.34	284					68.04
116	186.2	128.4	95.75	61.60	25.20	288					69.23
120	196.7	135.3	100.7	64.46	26.06	292					70.43
124		142.3	105.7	67.36	26.94	296					71.63
128		149.5	110.8	70.33	27.82	300					72.85
132		156.9	116.1	73.35	28.71	304					74.07
136		164.4	121.5	76.43	29.61	308					75.30
140		172.1	127.0	79.56	30.52	312					76.54
144			132.6	82.75	31.44	316					77.78
148			138.3	85.99	32.36	320					79.04
152			144.1	89.29	33.29	324					80.30
156			150.0	92.65	34.23	328					81.57
160			156.1	96.06	35.18	332					82.85
164				99.53	36.07	336					84.13
168				103.1	37.02	340					85.43
172				106.6	37.98						

[a] This table encompasses the energy intervals in which measurements were made. Ranges for higher energies or for other ions are found by taking λ from Table I and evaluating the range by using Eq. (4).

argument β/z, $M =$ mass of ion in proton mass units, and $z =$ atomic number of ion.

VI. RATES OF ENERGY LOSS AND EFFECTIVE CHARGE

Figure 6 shows the rate of energy loss dT/dR in Mev/μ as a function of ion and residual range. The curves were obtained by differentiating the least-squares polynomial fit to the experimental range-energy data. The dominant feature of each curve is the rise in $dT/dR = (z^{*2}/v^2)F(v)$ as the velocity decreases, reaching a maximum between 7 and 15 μ residual range, and its subsequent decrease owing largely to electron pickup. The points of maximum ionization correspond to the points of inflection in the range-energy curves in Fig. 3.

It is noted that the slopes of the range curves are not zero and therefore the dT/dR curves have finite values at zero range. The reasons for this result are as follows: First, we have defined zero range to be (on the average) the center of the last developed grain. Since the velocity of a particle is in general a power function of the range, the average velocity, and thus dT/dR, will not have an average value of zero at the center of the last grain. Second, and probably most important, as the velocity decreases, energy loss processes other than ionization—principally interactions with whole atoms—become dominant and give rise to energy losses that are not observable as developed grains.

We have defined the effective charge carried by an ion at velocity β as that charge which produces the observed rate of energy loss. The effective charge, z^*, is obtained from the ratio

$$\left(\frac{dT}{dR}\right)_\beta \bigg/ \left(\frac{d\tau}{d\lambda}\right)_\beta = z^{*2}(\beta), \qquad (5)$$

where dT/dR is the rate of energy loss of the ion and $d\tau/d\lambda$ is the rate of energy loss of the proton. It is appropriate to assert here that the effective charge, z^*, and the rms charge, z^{rms}, carried by the ion cannot be
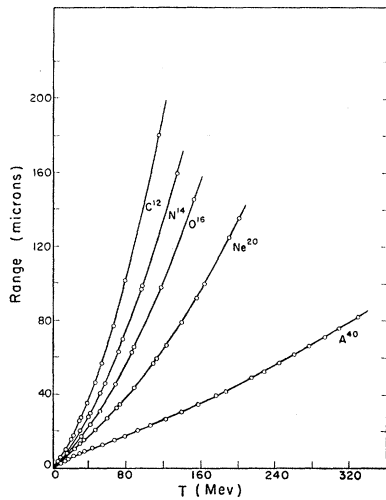
FIG. 3. Range-energy relations for C, N, O, Ne, and A ions in Ilford emulsion (3.815 g/cm³). The curves through the experimental points are the least-squares polynomials fitted to the data.
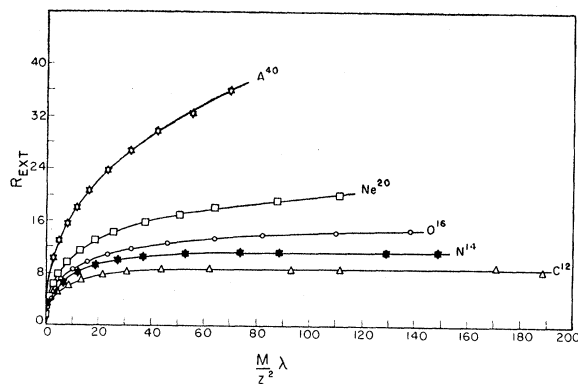

FIG. 4. Range extension, R_{ext}, attributable to the neutralization of the ionic charge as a function of $(M/z^2)\lambda$ for each type of ion. The quantity $(M/z^2)\lambda$ would be the range of the ion if no charge neutralization took place. The range of an ion is given by $R(\beta) = (M/z^2)\lambda(\beta) + R_{ext}$.

expected to be the same at the same velocity. In all probability z^* is greater than z^{rms}, owing to incomplete screening of the nucleus. The quantities z^* and z^{rms} are equal only if the electric field experienced by an electron of the stopping material at a distance r is $z'e/r^2$. This is not true for the electrons that penetrate the ion structure.

In Fig. 7, we have plotted the effective charge z^* divided by z as a function of the reduced velocity $\beta/z^{\frac{2}{3}}$. To augment our data at lower velocities we have included in Fig. 8 some results compiled from published data.[26] The stopping material in the work of Allison and Littlejohn, Lillie, and Weyl was air, while we have quoted the charge carried by fission fragments in neon gas.[31] Qualitatively, the experimental points form a

[31] C. B. Fulmer, Oak Ridge National Laboratory Report ORNL-2320 August, 1957 (unpublished).

locus that tends to justify the choice of $\beta/z^{\frac{2}{3}}$ as the velocity parameter to generalize the experimental results of z^*/z. For values of $z^*/z < 0.7$ the data are entirely consistent with the $\beta/z^{\frac{2}{3}}$ dependence, as predicted by the Fermi-Thomas (F-T) atomic model. However, at higher degrees of ionization, definite discrepancies appear. For instance, at $z^*/z = 0.9$ (see Fig. 7) it is observed that the values of $\beta/z^{\frac{2}{3}}$ increase monotonically with z of the ion. Such a variation with z indicates that the description of z^*/z at the higher degrees of ionization, and where the K electrons are involved, requires a reduced velocity parameter that approaches β/z; then the velocity of a K electron rather than that of the average electron is most important. If we assume the functional form for z^*/z to be of type $f(\beta/z^n)$, the charge index, n, can be evaluated from our experimental data. Figure 9 shows n as a function of z^*/z. The F-T statistical model predicts n to be $\frac{2}{3}$. However, in the region where the K electrons become important (and where a statistical model can no longer be valid) the experimental points clearly indicate that n does not remain constant, but approaches 1 as $z^*/z \rightarrow 1$.
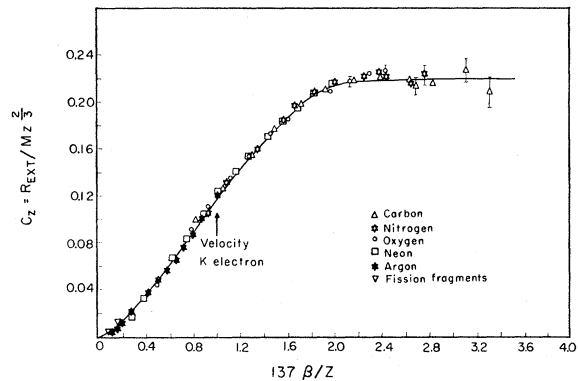

FIG. 5. Empirically derived universal curve relating $R_{ext}/Mz^{\frac{2}{3}}$ to the velocity of the ion in units of the K-electron velocity. The fission-fragment ranges are those given by L. Vigneron [Compt. rend. 231, 1473 (1950)].
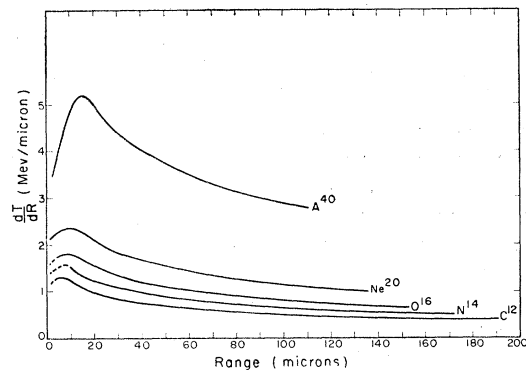

FIG. 6. The rate of energy loss as a function of residual range. The curves are dashed where they have been extrapolated to shorter ranges than were actually measured.
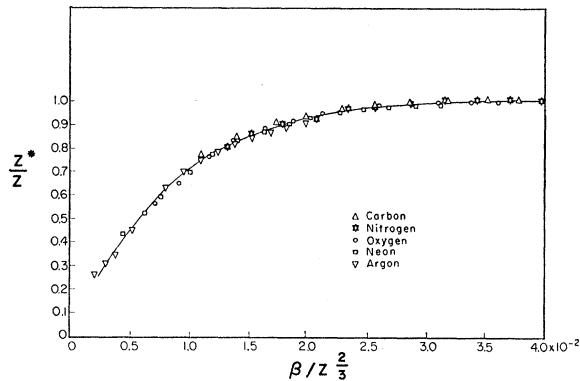
FIG. 7. The fractional effective charge, z^*/z, required to produce the observed rates of energy loss as a function of the reduced velocity of the ion, $\beta/z^{\frac{2}{3}}$.
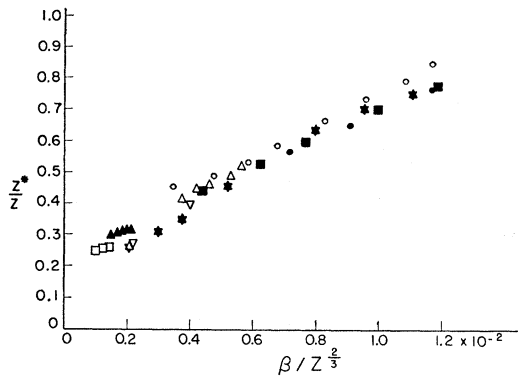

FIG. 8. Partial compilation of published data on z^*/z at low velocities for various ions and materials. Included from our data are low velocity points for O, Ne, and A ions. Key: $\triangle$ Li[7] (Allison and Littlejohn)[26] (in air); $\circ$ B[11] (Lillie)[26] (in air); $\blacktriangle$ N[14] (Weyl)[26] (in air); $\square$ Ne[20] (Weyl)[26] (in air); $\triangledown$ fission fragments (Fulmer)[31] (in neon); $\star$ A[40] (this experiment); $\blacksquare$ Ne[20] (this experiment); $\bullet$ O[16] (this experiment).

As mentioned previously, Papineau took as a basis the result of the F-T model and constructed a curve of z'/z vs $\beta/z^{\frac{2}{3}}$ from data on the charge distributions carried by ions after traversing argon gas or films of organic material. In Fig. 10, we reproduce these data as well as the fitted and extrapolated curve that Papineau deduced from the data. For comparison we also show the curve representing the locus of points from Fig. 5 obtained from this experiment. The differences between the observed ion ranges and those calculated by Papineau for $\beta/z^{\frac{2}{3}} > 1.5 \times 10^{-2}$ can be attributed to his use of values of z'/z that are systematically low relative to our experimental (z^*/z) curve. This difference leads to calculated ranges that are too long at the higher velocities. Below $\beta/z^{\frac{2}{3}} = 1.5 \times 10^{-2}$, the experimental values of z^*/z are well approximated by Papineau's curve, and the calculated and measured ranges are in closer agreement.

VII. DISCUSSION OF RANGE DATA

The range extension (R_{ext}) is functionally related to the effective charge (z^*/z) by the expression[29]

$$\frac{z^2}{M}R_{ext} = \int_0^\lambda \left[\left(\frac{z}{z^*} \right)^2 - 1 \right] d\lambda, \qquad (6)$$

or, in terms of velocity, β,

$$\frac{z^2}{M}R_{ext} = \int_0^\beta \left[\left(\frac{z}{z^*} \right)^2 - 1 \right] \left(\frac{d\lambda}{d\beta} \right) d\beta. \qquad (7)$$

From the measurements of the effective charge z^*/z and the range-velocity relation (for protons) $\lambda(\beta)$, one may be able to account for the observed dependence of R_{ext} upon the ion velocity in units of $z/137$. Unfortunately, a large contribution to the value of these
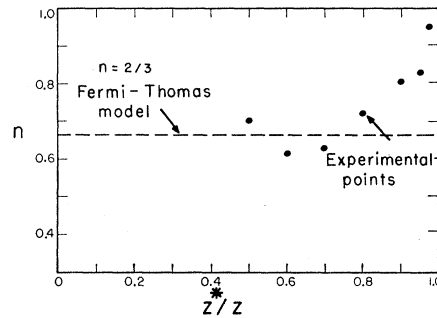

FIG. 9. Experimental values of the charge index, n, as a function of z^*/z, where n is defined by the equation $z^*/z = f(\beta/z^n)$.
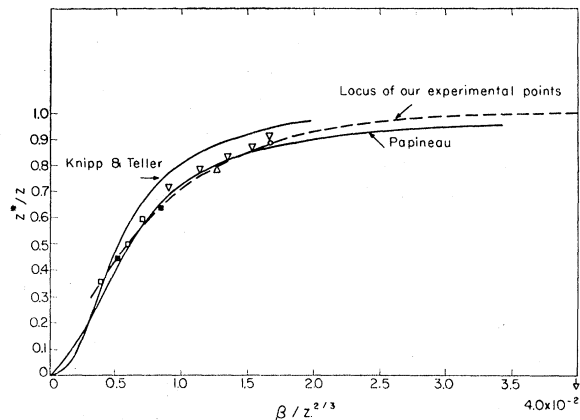

FIG. 10. Comparison of our experimental points of z^*/z with the curve deduced by Papineau from the experimental points shown, and the theoretical results obtained by Knipp and Teller. Key: $\blacksquare$ O[16] in argon, Hubbard and Lauer[20]; $\square$ Ne[20] in argon, Hubbard and Lauer[20]; $\circ$ N[14] in formvar, H. L. Reynolds and A. Zucker [Phys. Rev. **95**, 1353 (1954)]; $\triangledown$ N[14] in formvar, Reynolds, Wyly, and Zucker[18]; $\triangle$ N[14] in organic material, Stephens and Walker.[19] The points plotted from these data are actually evaluated from the rms value of the charge carried by the ion after traversing sufficient material to produce an equilibrium charge-state distribution. The curve derived by Knipp and Teller describes the velocity distribution of the electrons in a statistical model of the atom.

integrals occurs for the very low values of β where $\lambda \leqslant 2\mu$ and, likewise, for large values of $z/z^* \to \infty$. Even for argon, our data terminate when z/z^* has a maximum value of only 13; and the details of the range curve for protons less than 1 Mev ($\lambda < 14\mu$) are quite uncertain.

For these reasons efforts to derive a reliable analytic expression for R_{ext} by carrying out the integration of Eq. (6) and Eq. (7) have not been successful, but the following observations can be made regarding the functional form of the dependence of R_{ext} on M, z, and β:

(a) it is seen that a nearly universal function of the range extension is $R_{ext}/Mz^{\frac{3}{2}}$ when the independent variable is taken to be the velocity of the ion in units of $z/137$ (as shown in Fig. 5);

(b) the quantity $R_{ext}/Mz^{\frac{3}{2}}$, however, is slightly dependent directly upon the atomic number, z, of the ion, and hence no truly universal function of velocity can exist for $C_z \equiv R_{ext}/Mz^{\frac{3}{2}}$. This z dependence, unfortunately, is not fully revealed by our data. The effect would be observed most readily at velocities large enough to enable all of the ions to reach their asymptotic values of C_z. We should then expect to observe monotonically increasing values of C_z with atomic number.

In this experiment the maximum velocity was sufficient to allow only N^{14} and C^{12} to become totally stripped of electrons. Since N^{14} and C^{12} (and lighter ions) are stripped at relatively low velocities, the velocity interval over which the electron-capturing process takes place is small enough to permit $\lambda(\beta)$ to be approximated by the relation $\lambda = K\beta^{8/3}$. (In reference 29, β^3 was assumed.) For the light ions ($z \leqslant 7$), our results indicate that the K electron velocity ($z/137$) is the principal parameter that determinates the effective charge, z^*/z. We have used the data compiled by Whaling on the differential stopping cross section of the light ions ($z \leqslant 7$) in various stopping materials and have compared them with the stopping cross sections of protons at the same velocity. We have concluded, for these ions, that $z^*/z \approx f(\beta/z)$. With this argument,
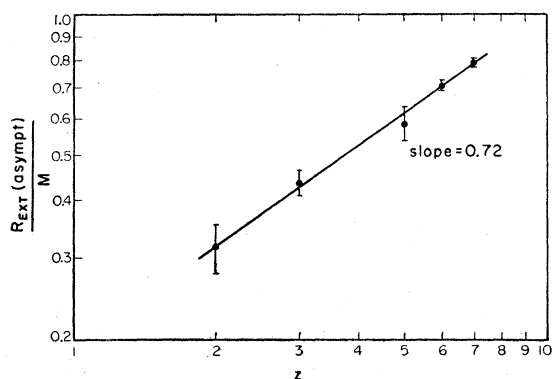
we may now write Eq. (6) as

$$\frac{z^2 R_{ext}}{M} = \int f(\beta/z) d\lambda.$$

Using the relation $\lambda \propto \beta^{8/3}$, we obtain $R_{ext}/Mz^{\frac{3}{2}} = F(\beta/z)$ $\equiv C_z$, which is the functional form the experimental data exhibit in Fig. 5.

We have shown, therefore, with quite reasonable approximations, that for the lighter ions the range extension is primarily a function of β/z. At velocities greater than about twice the K-electron velocity, when the ions are completely stripped, C_z becomes a constant and the R_{ext} is proportional to $z^{\frac{3}{2}}$. Figure 11 shows the asymptotic value of R_{ext}/M as a function of z for the ions of $z = 2$, 3, 5, 6, and 7. The R_{ext}/M measurement by Barkas for lithium and boron[29] has been included to supplement our data. The alpha-particle measurement was obtained in this experiment by comparing the
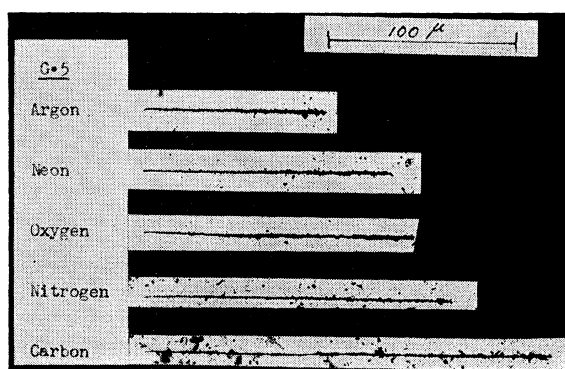

Fig. 12. Photomicrographs of stopping heavy-ion tracks in electron-sensitive $G5$ emulsion. The kinetic energies of the ions are about 10 Mev/nucleon. The particles traverse the emulsion from right to left.

ranges of our calibrating particles, alphas and protons, at the same $B\rho$. The slope drawn through the points is 0.72 ± 0.08, in close agreement with the estimated value of the charge exponent of $\frac{2}{3}$. Because it is sensitive to the range-velocity exponent, no fundamental significance can be attached to this value, however.

VIII. DISCUSSION OF QUALITATIVE FEATURES OF THE TRACKS PRODUCED BY HEAVY IONS

The charge of a stopping heavy ion is often estimated from measurements of mean track width or integrated track area, as a function of residual range. The "taper length" is also cited as an indication of the charge of the ion. The practical importance of the tapering track necessitates an understanding of the mechanisms by which the ions produce this characteristic effect. The processes that could lead to this effect are primary and secondary ionization (δ-ray formation) and electron pickup. To deduce the relative importance of these

Fig. 11. Asymptotic values of R_{ext}/M as a function of atomic number. The Li and B points are from reference 29.

processes by analysis of the tracks themselves is difficult, and investigators of this problem have not all agreed in their conclusions.

As previously mentioned, we exposed a series of emulsions of different sensitivities to each type of ion. A qualitative study of these emulsions has enabled us to formulate some conclusions pertaining to the fundamental process involved that produces the tapering of heavy-ion tracks. First, we demonstrate in Fig. 12 the typical appearance of each type of ion track in an electron-sensitive emulsion (G5). Each of the ions has an energy of about 10 Mev/nucleon. The profiles of the stopping heavy ions clearly indicate that the tapering is dependent upon the nuclear charge, and that the over-all effect diminishes with decreasing charge. In each case, however, the tracks are devoid of any visual evidence of increase in the rate of ionization as the particle velocity decreases. We may compare
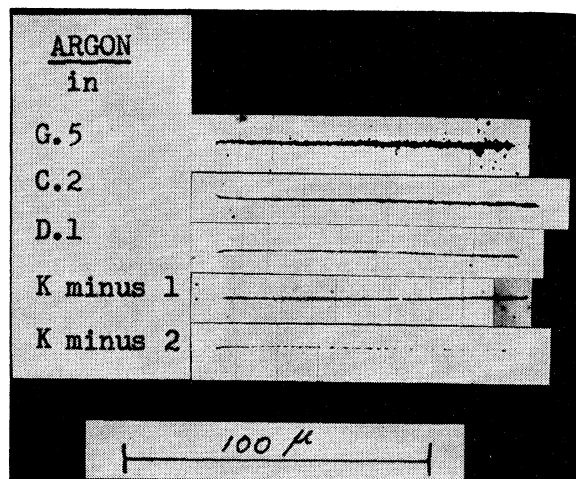
FIG. 13. Photomicrographs of 400-Mev argon ions in Ilford nuclear-track emulsion of various sensitivities.

the measured values of dT/dR as a function of residual range, shown in Fig. 6, with the photomicrographs of Fig. 12. We see there is little or no correlation between the track width for the ion and the actual rate of energy loss experienced by the particle. Whereas the track widths monotonically decrease with decreasing range (from which one might suspect that decrease of ionization is really due to electron pickup), the dT/dR curves show that the ionizations of all the ions increase with decreasing velocity until the last 7 to 15 microns of range. In this region the rates of ionization reach a maximum and then decrease as the ion undergoes its final phase of neutralization. In order to demonstrate the differences between emulsions of different sensitivities, the tracks of argon (in $G5$, $C2$, $D1$, K minus 1, and K minus 2) are reproduced in Fig. 13. It is not until the most insensitive emulsion, K minus 2, is reached, that the influence of the δ-ray electrons on the
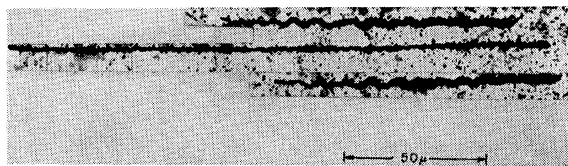

FIG. 14. Example of buckling-type distortions in tracks of heavily ionizing particles. The distorted (corkscrew) tracks are those of argon ions; the adjacent nondistorted track is a neon ion. These tracks were observed in uranium-loaded C2 emulsions. The buckling distortions have also been produced in nonloaded emulsions that have undergone long development times in D-19.

track profile is essentially eliminated. The primary ionization becomes the dominant process that determines the visual characteristics of the track. The grain density along the argon track in the insensitive emulsion parallels the curve for measured dT/dR vs range for argon.

From these data one can attribute the tapering of multicharged ion tracks to the δ-ray production along the track. The track width at a given point is predominantly determined by the spatial distribution of the energetic δ rays, and the tapering of the track toward lower ion velocities is due to the decreasing energies (and therefore the "diffusion" length from the core of the track) of the fastest δ rays. It should be mentioned that for argon, in particular, electron pickup occurs throughout the entire observed range ($\beta_{max} \approx z/137$). However, the rate of neutralization of the ion does not dominate the velocity dependence of dT/dR until the last 15 microns of the track. We conclude that the tapering of heavy-ion tracks in electron-sensitive emulsion cannot be satisfactorily interpreted as the consequence of the diminution of the charge of the ion, but is due primarily to the copious production of δ rays along the track. Our observations therefore fully confirm the conclusion of several recent investigations of this point.[32]

In the course of an experiment dealing with fission processes induced in uranium by fast argon beams, Muga brought to our attention a type of track distortion that we had not observed before.[33] The tracks of argon in the uranyl-nitrate-loaded plates were so buckled that they had all the characteristics of an irregular "corkscrew." The distortions are dramatically reproduced in Fig. 14. In a plate furnished us by Muga, we have photographed a distorted argon track that is adjacent to a neon track that does not show evidence of distortion at all. Shapiro has informed us that these distortions have been observed earlier in studies of the heavy-nuclei component of the primary cosmic radiation, although they were generally considered to arise from emulsion shrinkage upon processing.[34] The par-

[32] P. G. Bizzeti and M. Della Corte, Nuovo cimento 11, 317 (1959).

[33] Luis Muga (private communication).

[34] M. M. Shapiro (private communication), and Trans. N. Y. Acad. Sci. 20, 697 (1958).
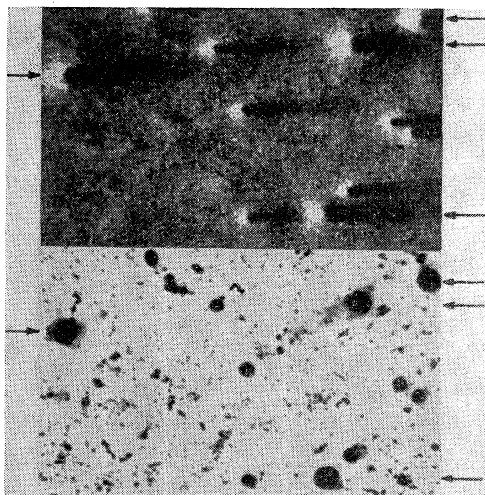
FIG. 15. Photomicrographs of argon and carbon tracks that enter normal to the emulsion (G5) surface. On the left, the tracks are photographed as they appear "end-on" in the microscope using transmitted light. The argon ions (4) are denoted by the arrows; the carbon tracks (7) are approximately one-half the diameter of the argon tracks. On the right, the same group of ions is photographed, but with the illumination coming from light scattered by the surface from a pencil of light placed at grazing incidence to the surface. The tracks, as "columns of silver," protrude above the surface (5 μ for A, 3 μ for C) as evidenced by the shadows they cast.

ticles in Fig. 14 entered the emulsion surface at a small enough dip (about 5°) so that the influence of emulsion shrinkage is largely eliminated. The only difference between the tracks that could explain the observed effect is the difference between the rates of energy loss of the argon and neon ions. If the buckling of the tracks is caused by physical development, then one should expect to observe the growth of these distortions simply by varying the time of development in a suitable physical-developing solution. Several G5 emulsions were exposed to all ions; the beams entered at a 5° dip angle. The plates were differentially developed in 10-minute intervals from 10 to 120 minutes in D-19 developer (diluted 6:1) at 22°C. The argon tracks began to buckle after a developing time of 50 minutes. The initial states of the distortion were observed to be concentrated in the regions of maximum ionization of the track. After about 90 minutes, the argon tracks were completely distorted to shapes similar to that in Fig. 14. In these development tests, we did not observe as extreme effects as demonstrated in the photograph. However, the fact that "corkscrews"

were manufactured by strong development alone indicates that the distortions are only enhanced by metallic additives such as uranium to the emulsion. Actually, corkscrew distortions had been produced in the tracks of all ions by the time the 2-hour developing test was completed, although the carbon tracks were only in the early stages of deformation.

A possible explanation for this phenomenon of track buckling is that when a large fraction of the silver halide crystals has been rendered developable, the growth of the developing crystals caused by deposition of metallic ions from the developing bath leaves insufficient room for all the grains to remain along the particle trajectory. Instead of individual grains being displaced, the whole particle trajectory is buckled as if the grains had some coherence.

We conclude this discussion of the physical characteristic of tracks of heavily ionizing particles ($dT/dR \rightarrow$ 50 Bev/cm), by referring to Fig. 15. Here we show, by two different types of illumination, tracks of argon and carbon that enter normal to the surface of a G5 emulsion. The photomicrograph (a) on the left shows the appearance of the tracks, looking end-on at the top surface of the emulsion, using transmitted light. On the right (b) is the same field of view with a pencil of light at grazing incidence illuminating the emulsion surface. The "rigid columns" of silver produced by the argon and carbon ions clearly protrude above the surface of the processed emulsion (1 hour in D-19), as evidenced by the shadows they cast. The largest protrusions are argon tracks that extend about 5 μ above the surface; the smaller ones are carbon tracks that extend some 3 μ above the surface. Because the tracks were able to extend above the surface of the shrinking emulsion during drying, the "columns" of silver were sufficiently relieved of compressive forces so that no lateral buckling of the tracks was detected.
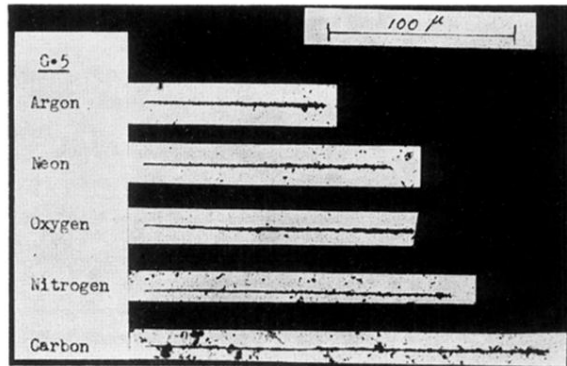
ACKNOWLEDGMENTS

Fig. 12. Photomicrographs of stopping heavy-ion tracks in electron-sensitive G5 emulsion. The kinetic energies of the ions are about 10 Mev/nucleon. The particles traverse the emulsion from right to left.
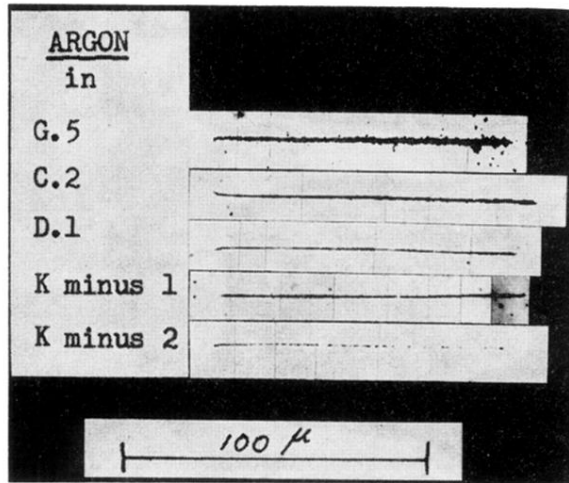
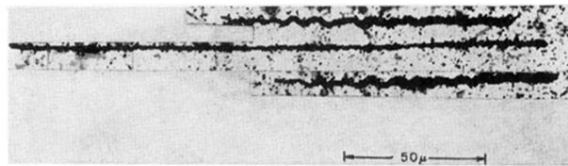FIG. 13. Photomicrographs of 400-Mev argon ions in Ilford nuclear-track emulsion of various sensitivities.

FIG. 14. Example of buckling-type distortions in tracks of heavily ionizing particles. The distorted (corkscrew) tracks are those of argon ions; the adjacent nondistorted track is a neon ion. These tracks were observed in uranium-loaded C2 emulsions. The buckling distortions have also been produced in nonloaded emulsions that have undergone long development times in D-19.
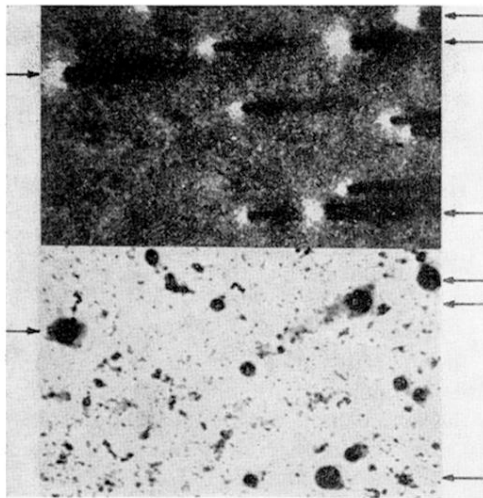
FIG. 15. Photomicrographs of argon and carbon tracks that enter normal to the emulsion (G5) surface. On the left, the tracks are photographed as they appear "end-on" in the microscope using transmitted light. The argon ions (4) are denoted by the arrows; the carbon tracks (7) are approximately one-half the diameter of the argon tracks. On the right, the same group of ions is photographed, but with the illumination coming from light scattered by the surface from a pencil of light placed at grazing incidence to the surface. The tracks, as "columns of silver," protrude above the surface (5 μ for A, 3 μ for C) as evidenced by the shadows they cast.